

Combustion synthesis and structural characterization of Li–Ti mixed nanoferrites

R M SANGSHETTI[†], V A HIREMATH^{††} and V M JALI^{*}

Department of Physics, Gulbarga University, Gulbarga 585 106, India

[†]Department of Physics, ^{††}Department of Chemistry, P.D.A. College of Engineering, Gulbarga 585 102, India

MS received 26 October 2010; revised 9 March 2011

Abstract. Polycrystalline samples of the mixed nanoferrites, $\text{Li}_{0.5+0.5x}\text{Ti}_x\text{Fe}_{2.5-1.5x}\text{O}_4$ ($0.02 \leq x \leq 0.1$), were prepared by combustion method at lower temperatures compared to the conventional high temperature sintering for the first time at low temperatures, using PEG which acts as a new fuel and oxidant. XRD patterns reveal a single-phase cubic spinel structure. The as synthesized Li–Ti ferrites are in nanocrystalline phase. The crystallite size was found to be in the range 16–27 nm. SEM images reveal rod-like morphology in all the samples with a discontinuous grain growth. The B–H loops have been traced using VSM technique, for all the compositions, at room temperature and the hysteresis parameters are calculated. Saturation magnetization decreases with increase in Ti content due to the fact that the Ti^{4+} ion, which is a non-magnetic ion, replaces a magnetic Fe^{3+} ion. The hysteresis loops show clear saturation at an applied field of ± 10 kOe and the loops are highly symmetric in nature. The cation distribution is known indirectly by using saturation magnetization values.

Keywords. Li–Ti mixed ferrites; combustion synthesis; hysteresis.

1. Introduction

Lithium ferrites are low cost materials, which are generally found useful in microwave-device and memory-core applications (Baba and Argentina 1975; Dionne 1975; Kulshreshtha and Ritter 1985; Bermejo *et al* 1994). The modifications in the properties of ferrites due to substitution of different ions, those dependent upon the nature and number of substituted ions, have been studied by various workers. Several studies (Watanabe *et al* 1981; Gill and Puri 1985; Reddy *et al* 1988) have been reported with additions of divalent, trivalent and tetravalent ions to monitor various parameters, depending on the desired applications of ferrites. Non-magnetic substitution in ferrites alter the inter and intra-sub lattice exchange interactions between the magnetic ions giving rise to a variety of interesting magnetic properties (Neel 1951). Substitution of non-magnetic ions weakens the exchange interaction and can lead to the formation of paramagnetic clusters (Gilleo 1960), localized canting (Nicolas *et al* 1973), etc altering the net magnetic moment. A study of magnetization is useful in understanding the arrangement of spins and the distribution of magnetic cations in the sublattice. On the other hand, mixed lithium ferrite

has been used as a promising substitute for NiCuZn ferrites for advanced planar ferrite devices, such as multilayer chip inductors (MLCIs), because of their low sintering temperature, high Curie temperature and excellent electromagnetic properties at high frequency (Zhou *et al* 1998).

It is well known that low temperature sintering of ferrites can be achieved by using active ultrafine powders synthesized via a wet chemical method. Several chemical processing techniques, such as hydrothermal, sol–gel, coprecipitation and combustion synthesis have been investigated to prepare ultrafine ferrite powders (Fujimoto 1994; Dias and Buono 1997; Ravindranathan and Patil 1987; Kumar *et al* 1996; Suresh and Patil 1992; Cho *et al* 1999). Among these techniques, combustion synthesis has been proved to be a simple and economic way to prepare nanoscale powders (Chakrabarti and Maiti 1997; Schafer *et al* 1997; Yue *et al* 1999). In this technique, a thermally induced redox reaction takes place and the reaction is exothermic. The energy from the exothermic reaction between oxidant and reductant can be high enough to form a desirable phase within a very short time. High temperature synthesis of Li ferrites involves volatilization of lithium and oxygen at a temperature above 1000°C, which affects the magnetic properties (White and Patton 1978). In view of this, to reduce the loss of lithium content, an attempt has been made to synthesize the Li–Ti mixed ferrites employing combustion synthesis, at different compositions, at a reduced temperature of sintering compared to the conventional high

*Author for correspondence (vmjali@gmail.com)

temperature synthesis routes reported in literature (Reddy *et al* 1988; Wafik *et al* 1993).

2. Experimental

Li–Ti mixed ferrites with the compositional formula, $\text{Li}_{0.5+0.5x}\text{Ti}_x\text{Fe}_{2.5-1.5x}\text{O}_4$ ($0.02 \leq x \leq 0.1$), were prepared by combustion method using high-purity analytic reagents LiCO_3 , Fe_2O_3 , TiO_2 and polyethylene glycol (PEG). PEG (molecular weight, 6000) acts as a new fuel for combustion synthesis. All the initial reagents were mixed with PEG in a weight ratio of 1:2 and ground well in a pestle and mortar. The resulting mixture was placed in an alumina crucible and sintered at a temperature of 350°C for 3 h. The reacted powders were ball milled with distilled water as wetting agent for 5 h and dried. Phase confirmation and structure determination were done using X-ray diffraction (XRD, Philips PW 1051). The structure and lattice parameter values were obtained using the ‘POWDER X’ software. Scanning electron microscope was used to study the powder surface morphology (SEM, Leica - 440 Cambridge Stereoscan). The average crystallite size was calculated by the well known Scherrer’s equation. Vibrating Sample Magnetometer (VSM, Quantum model - VSM 6000) at an applied field of ± 10 kOe was used for study of magnetization. Small amounts of the sample (0.05 g) were placed in a glass ampoule of 1 mm inner diameter and mounted in VSM. The magnetization variation was studied as a function of magnetic field at room temperature for all compositions and hysteresis parameters were calculated.

3. Results and discussion

3.1 Synthesis

Combustion synthesis, which is a quick and straightforward preparation process to produce homogeneous, crystalline and unagglomerated multi component oxide ceramic powders without the intermediate decomposition and/or calcining steps, was used to prepare Li–Ti mixed nanoferrites. These samples were successfully prepared for the first time at lower temperatures compared to conventional high temperature sintering, by combustion method using PEG which acts as a new fuel and oxidant.

3.2 Structural characterization

Figure 1 shows the comparison of XRD patterns of $\text{Li}_{0.5+0.5x}\text{Ti}_x\text{Fe}_{2.5-1.5x}\text{O}_4$ ($0.02 \leq x \leq 0.1$) samples in the $20\text{--}70^\circ$ 2θ range. The main reflection planes appear in all patterns. XRD analysis shows the single-phase cubic spinel structure and was confirmed by indexing all major peaks with ‘POWDER X’ software and lattice constant for all compositions was found to be 0.833 nm which is consistent with

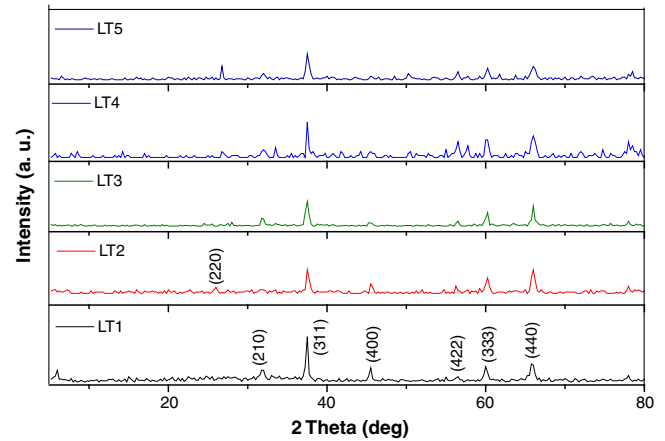


Figure 1. Comparison of XRD pattern of LT1 to LT5 samples at room temperature.

those reported by Yousif *et al* (1994). The theoretical lattice constants (a_{th}) were estimated from the ionic radii of the A sites (r_A), B sites (r_B) and the radius of oxygen ion (r_O) (Mazen *et al* 1993) using

$$a_{\text{th}} = (8/3\sqrt{3}) [(r_A + r_O) + \sqrt{3}(r_A + r_O)].$$

These theoretical lattice parameter values were found to be 0.833 nm. These values are consistent with those reported by Yousif *et al* (1994). The crystallite sizes of the synthesized powders were determined using Scherrer’s equation

$$D = \frac{0.9\lambda}{\beta \cos \theta},$$

where D is particle size, λ the wavelength of $\text{CuK}\alpha$, β the FWHM and θ the diffraction angle.

Table 1 shows the average crystallite size, saturation magnetization and coercivity values. The synthesized powders have nanocrystalline particles with crystallite size, 16–27 nm.

3.3 Microstructure analysis

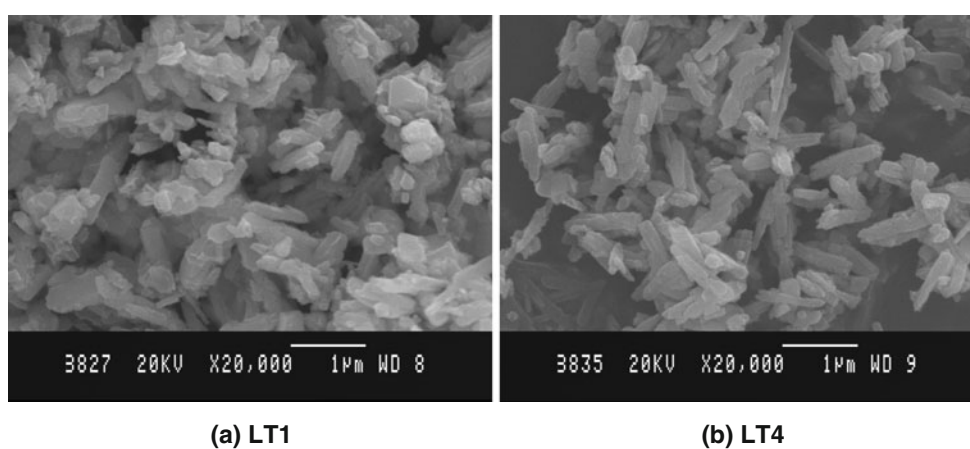
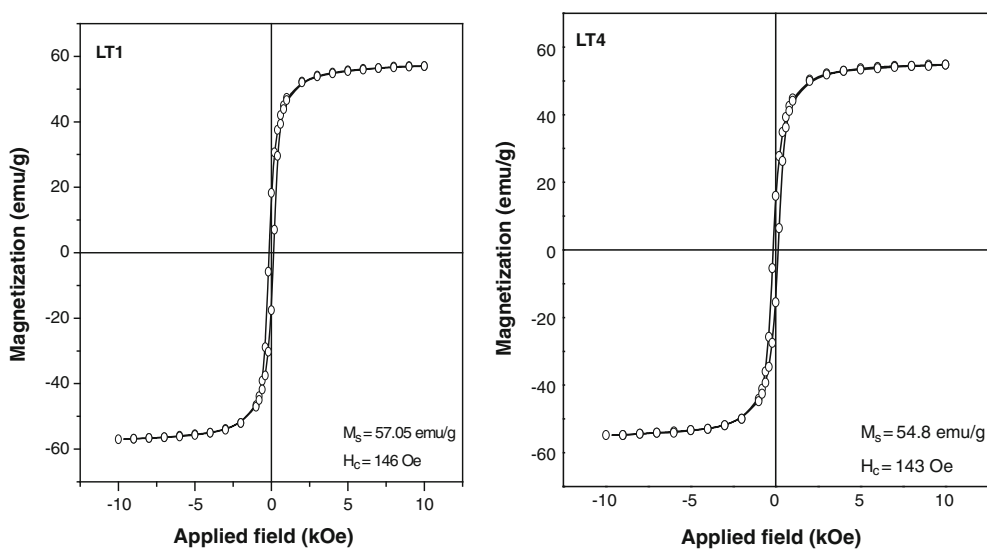
Figure 2 shows SEM images at a magnification of $\times 20\text{K}$ of LT1 and LT4 samples. Rod-like morphology was observed in all the samples with discontinuous grain growth. No other different morphological grains were observed indicating that no second phase was present.

3.4 VSM

The primary function of Ti is to lower saturation magnetization (M_s) value. As in all ferrites, the magnetization may be reduced by the substitution of various non-magnetic

Table 1. Crystallite size, saturation magnetization and coercivity values.

Ferrite	Sample code	Crystallite size (nm)	Saturation magnetization, M_s (emu/g)	Coercivity, H_c (Oe)
$\text{Li}_{0.5+0.5x}\text{Ti}_x\text{Fe}_{2.5-1.5x}\text{O}_4$ ($x = 0.02$)	LT1	19.59	57.05	146
$\text{Li}_{0.5+0.5x}\text{Ti}_x\text{Fe}_{2.5-1.5x}\text{O}_4$ ($x = 0.04$)	LT2	22.08	56.40	144
$\text{Li}_{0.5+0.5x}\text{Ti}_x\text{Fe}_{2.5-1.5x}\text{O}_4$ ($x = 0.06$)	LT3	16.13	55.00	180
$\text{Li}_{0.5+0.5x}\text{Ti}_x\text{Fe}_{2.5-1.5x}\text{O}_4$ ($x = 0.08$)	LT4	26.88	54.80	143
$\text{Li}_{0.5+0.5x}\text{Ti}_x\text{Fe}_{2.5-1.5x}\text{O}_4$ ($x = 0.10$)	LT5	19.06	52.96	137


Figure 2. SEM images of LT1 and LT4 samples at room temperature.

Figure 3. VSM curves for LT1 and LT4 samples at room temperature.

ions for Fe ions in the octahedral sublattice (Baba *et al* 1972). Figure 3 shows VSM curves for LT1 and LT4 samples, at room temperature. Magnetization values were obtained using vibrating sample magnetometer (VSM) and are shown in table 1 for different Ti contents. M_s value decreases with increase in Ti content due to the fact that the Ti^{4+} ion, which is a non-magnetic ion, replaces a magnetic Fe^{3+} ion. The variation of saturation magnetization with dopant concentration is shown in figure 4. It can be seen from the figure that the values of saturation magnetization decreases with increase in Ti concentration. The coercivity value decreases with increase in Ti-content except in LT3 sample. We cannot establish clearly the inverse nature of coercivity with crystallite size. The hysteresis loops show clear saturation at an applied field of ± 10 kOe. The loops are highly symmetric

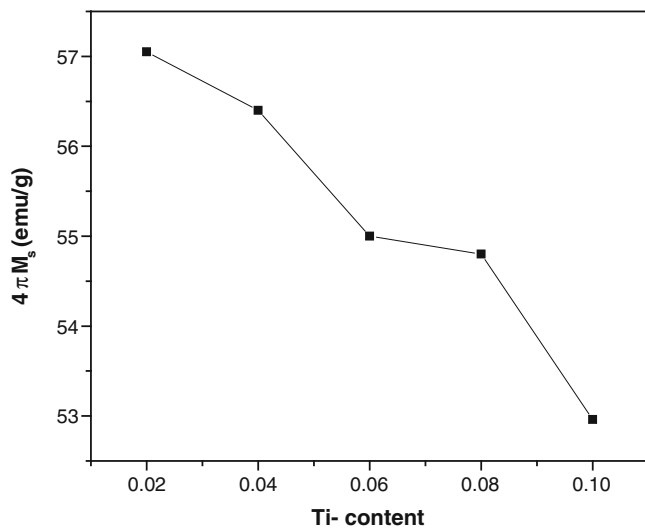


Figure 4. Variation of saturation magnetization with Ti-content.

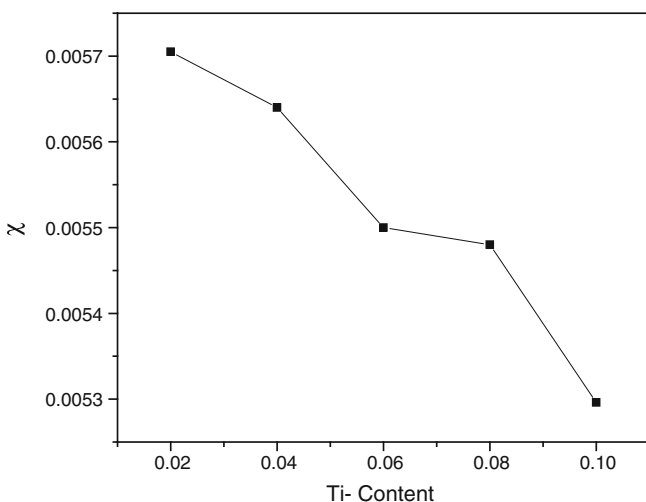


Figure 5. Variation of magnetic susceptibility with Ti-content.

in nature. Magnetic susceptibility (M/H) decreases with increase in Ti-content and is as shown in figure 5.

4. Conclusions

Li-Ti mixed ferrites were synthesized at different compositions at a reduced temperature of sintering compared to the conventional high temperature synthesis. XRD pattern reveals a single-phase cubic spinel structure. The results revealed that the nanocrystalline Li-Ti ferrite powders directly formed after combustion and that the products' properties showed good reproducibility. SEM images reveal rod-like morphology with discontinuous grain growth. The saturation magnetization value decreases with increase in Ti content due to the fact that the Ti^{4+} ion, which is non-magnetic, replaces a magnetic Fe^{3+} ion. For ferrite application in recording media, low coercivity is required while maintaining high saturation magnetization. In the present case, however, coercivity has been lowered due to Ti substitution without maintaining high saturation magnetization. As Ti^{4+} is diamagnetic in nature, this observation is expected. As it is well known, squareness of hysteresis loop has attracted considerable attention. The present study also presents such squareness of the hysteresis loops. Following the work by Argentina and Baba (1974), when titanium ions are introduced in lithium ferrite, as the saturation magnetization value is found to decrease with increasing Ti content, it can be concluded that these Ti dopants may occupy the octahedral sites replacing Fe^{3+} ions.

References

- Argentina G M and Baba P D 1974 *IEEE Trans. Micr. Theory Tech.* **MTT-22** 652
- Baba P D and Argentina G M 1975 *IEEE Trans. Microwave Theory Tech.* **22** 654
- Baba P D, Argentina G M, Courtney W E, Dionne G F and Temme D H 1972 *IEEE Trans. Magn.* **MAG-8** 83
- Bermejo E, Chassing J, Bizot D and Quarton M 1994 *Mater. Sci. Eng.* **B22** 73
- Chakrabarti N and Maiti H L 1997 *Mater. Lett.* **30** 169
- Cho Y S, Burdick V L and Amarakoon V R W 1999 *J. Am. Ceram. Soc.* **82** 1416
- Dias A and Buono V T 1997 *J. Mater. Res.* **12** 3278
- Dionne G F 1975 *J. Appl. Phys.* **45** 3621
- Fujimoto M 1994 *J. Am. Ceram. Soc.* **77** 3065
- Gill N K and Puri R K 1985 *J. Mater. Sci. Lett.* **4** 396
- Gilleo M A 1960 *J. Phys. Chem. Solids* **13** 33
- Kulshreshtha S K and Ritter G 1985 *J. Mater. Sci.* **20** 3926
- Kumar P S A, Shrotri J J and Kulkarni S D 1996 *Mater. Lett.* **27** 293
- Mazen S A, Abdalla M H, Nakhla R I, Zaki H M and Metawe F 1993 *Mater. Chem. Phys.* **34** 35
- Neel L 1951 *J. Phys. Radium* **12** 160
- Nicolas J, Lagrange A, Sroussi R and Inglebert R L 1973 *IEEE Trans. Mag.* **MAG-9** 546

- Ravindranathan P and Patil K C 1987 *Am. Ceram. Soc. Bull.* **66** 688
- Reddy P V, Reddy M B, Muley V N and Ramana Y V 1988 *J. Mater. Sci. Lett.* **7** 1243
- Schafer J, Sigmand W, Roy S and Aldinger F 1997 *J. Mater. Res.* **12** 2518
- Suresh K and Patil K C 1992 *J. Solid State Chem.* **99** 12
- Watanabe A, Yamamura H, Moriyoshi Y and Shirasaki S 1981 *Ferrites, proc. int. conf. Tokyo, Japan* (eds) H Watanabe *et al* (Tokyo: Centre for Academic Publications) p. 170
- Wafik A H, Mazen S A and Mansour S F 1993 *J. Phys. D: Appl. Phys.* **26** 2010
- White G O and Patton C E 1978 *J. Magn. Magn. Mater.* **9** 299
- Yousif A A, Elzain M E, Mazen S A, Sutherland H H, Abdalla M H and Masour S F 1994 *J. Phys.: Condens. Matter* **6** 5717
- Yue Z, Li L, Zhou J, Zhang H and Gui Z 1999 *Mater. Sci. Eng.* **B64** 68
- Zhou J, Liang B, Zhang H, Yun Zi, Gui Z and Li L 1998 *High Tech. Lett.* **8** 39